Microvascular Changes in the Choriocapillaris of Diabetic Patients Without Retinopathy Investigated by Swept-Source OCT Angiography

Yining Dai,[1] Hao Zhou,[1] Zhongdi Chu,[1] Qinqin Zhang,[1] Jennifer R. Chao,[2] Kasra A. Rezaei,[2] and Ruikang K. Wang[1,2]

[1]Department of Bioengineering, University of Washington, Seattle, Washington, United States
[2]Department of Ophthalmology, University of Washington Eye Institute, Seattle, Washington, United States

Correspondence: Ruikang K. Wang, Department of Bioengineering, University of Washington, 3720 NE 15th Avenue, Seattle, WA 98195, USA;
wangrk@uw.edu.

Received: July 5, 2019
Accepted: January 21, 2020
Published: March 30, 2020

Citation: Dai Y, Zhou H, Chu Z, et al. Microvascular changes in the choriocapillaris of diabetic patients without retinopathy investigated by swept-source OCT angiography. *Invest Ophthalmol Vis Sci.* 2020;61(3):50.
https://doi.org/10.1167/iovs.61.3.50

Purpose. To investigate the microvascular changes in macular retina and choriocapillaris (CC) in diabetic eyes without retinopathy using swept-source optical coherence tomography angiography (SS-OCTA).

Methods. A commercial SS-OCTA system was used to collect 6 × 6-mm macular scans from patients. Three depth-resolved retinal slabs and a CC slab were segmented by a validated semiautomated algorithm. Retinal vessel area density, vessel skeleton density, and nonperfusion area were calculated on segmented retinal slabs. Foveal avascular zone was automatically measured based on en face image of the whole retinal layer. For CC quantification, the percentage of flow deficits (FD%) and the flow deficit (FD) sizes were measured.

Results. Sixteen eyes from 16 diabetic patients without clinically detectable retinopathy and 16 eyes from 16 age-matched nondiabetic controls were included. There was no significant difference between the two groups in all retinal vessel quantitative parameters (all $P > 0.05$). However, the mean FD% and mean FD sizes were significantly increased in CC in the central 1.0-mm disk ($P = 0.011$ and $P = 0.017$, respectively), the central 1.5-mm rim ($P = 0.003$ and $P = 0.009$, respectively), the central 2.5-mm rim ($P = 0.018$ and $P = 0.020$, respectively), and the entire 5.0-mm disk ($P = 0.009$ and $P = 0.008$, respectively) in diabetic eyes compared with controls.

Conclusions. CC perfusion in the macula is decreased in diabetic patients without retinopathy as compared to age-matched normal controls. Decreased CC perfusion in the macula may be an early indicator of otherwise clinically undetectable diabetic vasculopathy.

Keywords: choriocapillaris, diabetic retinopathy, flow deficits, swept-source OCT angiography

Diabetic retinopathy (DR) is a common microvascular complication of diabetes mellitus (DM) and remains the leading cause of vision loss worldwide in the working-age population.[1–3] Therapeutic intervention is currently targeted toward treating complications resulting from irreversible structural changes in retinal vasculature. Early detection of the vascular abnormalities in diabetic eyes could provide timely recognition and management of patients at high risk of development of DR and progression.[4] The pathogenesis of DR is primarily attributed to vascular abnormalities in the retina.[5] Since the choroid is a vascular layer that supplies the outer retina, the potential effects of choroidal blood flow on the pathophysiology of DR have attracted increasing attention.[6] A few studies using indocyanine green angiography (ICGA) have shown choroidal abnormalities in eyes with DR.[7–9] Selective filling of the choriocapillaris (CC) on ICGA is speculated to represent the existence of early diabetic choroidopathy.[9] However, due to insufficient lateral resolution and lack of depth-resolved information of ICGA,[10] the delineation and quantification of CC flow in vivo are not attainable.

Optical coherence tomography (OCT) is a noninvasive imaging modality that has been widely applied in ophthalmic imaging.[11] With the development of OCT angiography (OCTA), blood flow can now be visualized in vivo with depth-resolved capability of the retinal and choroidal circulation in a rapid fashion.[12] While retinal vasculature imaging using OCTA is well documented in those with diabetic retinopathy, few studies have investigated blood flow in the CC in the same population of patients. Several groups have reported either normal or abnormal CC perfusion in diabetic eyes without DR by using spectral-domain OCTA (SD-OCTA).[13–16] However, one of the limitations of SD-OCTA is its shorter laser wavelength, which is more strongly

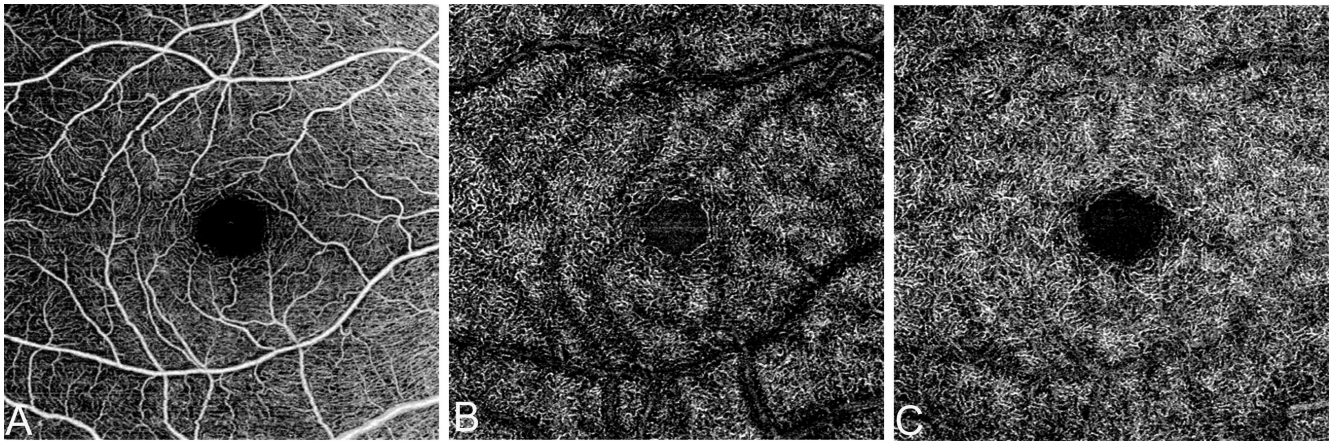

Figure 1. En face OCTA images of three retinal layers: (**A**) SRL, (**B**) IRL, and (**C**) DRL.

scattered by the retinal pigment epithelium (RPE), resulting in significant sensitivity loss when imaging structures beneath the RPE, such as the CC.[17] Swept-source OCTA (SS-OCTA), with a longer laser wavelength, has proven to be less affected by the RPE, allowing for more reliable visualization and detection of the CC.[17]

This study is designed to investigate quantitative changes in the flow impairment of both the retina and CC in diabetic patients without retinopathy. In doing so, we employed a commercially available SS-OCTA instrument to collect the OCTA imaging data from enrolled patients for analyses.

Methods

Participants

In this study, patients with a diagnosis of DM without DR, as determined by clinical examination and fundus imaging, and age-matched patients without a history of DM in the Department of Ophthalmology at the University of Washington Eye Institute in Seattle between January 2017 and June 2018 were retrospectively analyzed. This study adhered to the tenets of the Declaration of Helsinki and was performed in accordance with the Health Insurance Portability and Accountability Act. Ethical approval was obtained from the Institutional Review Board of the University of Washington. All enrolled participants provided written informed consent. Exclusion criteria were eyes with known ocular diseases such as retinal or choroidal pathology, glaucoma, uveitis, a refractive error of less than –6.0 diopters, prior intraocular surgery, and systemic diseases that might affect the retina or choroid, such as uncontrolled hypertension, systemic lupus erythematosus, anemia, and leukemia. Clinical and demographic characteristics were obtained from electronic medical records.

Imaging and Image Processing

Study participants were imaged with SS-OCTA with a 100-kHz A-line rate at 1060 nm (PLEX Elite 9000; Carl Zeiss Meditec, Inc, Dublin, CA, USA). A 6 × 6-mm (nominal) scan in the central macula was performed, consisting of 500 horizontal A-lines at 500 vertical locations with two repeated scans in each fixed location, resulting in a sampling spacing of 12 µm. The complex optical microangiography algorithm was used to obtain OCTA images.[18] Retinal and CC layers were segmented using a validated semiautomated segmentation algorithm,[19] and manual corrections were carried out as necessary to ensure accurate segmentation. The right eye was selected for analyses in the study unless gross eye movements or poor signal was noted. Images were excluded from the study if signal strength was less than seven as defined by the manufacturer or if there was severe motion artifact.

The retina was segmented into three depth-resolved layers (slabs) to better visualize vascular plexuses (Fig. 1)[20,21]: the superficial retinal layer (SRL), which is a slab extending from the inner limiting membrane to the superficial portion of the inner plexiform layer (IPL); the intermediate retinal layer (IRL) extending from the deep portion of IPL to the superficial portion of the inner nuclear layer (INL); and the deep retinal layer (DRL) extending from the deep portion of INL to the outer plexiform layer. The retinal vascular plexuses of the nerve fiber layer, the ganglion cell layer, and the superficial portion of IPL were grouped together because these layers could not be accurately assessed in the foveal region.[22] The vascular projection artifacts presented in the IRL and DRL slabs were removed using a previously published algorithm.[23]

The vessel area density (VAD), vessel skeleton density (VSD), foveal avascular zone (FAZ) area, and nonperfusion area (NPA) were calculated from the en face angiograms using our previously described method.[24–26] The VAD, VSD, and NPA were calculated on three retinal layers in the rim with inner and outer ring diameters of 1.0 and 2.5 mm ($R_{1.5}$, or parafovea) and the rim with inner and outer ring diameters of 2.5 and 5.0 mm ($R_{2.5}$, or perifovea) (Fig. 2). The FAZ was automatically measured based on en face images of the whole retinal layer.

The flow deficits (FDs) were measured by using our previously described method.[27] The CC was defined as a slab from the outer boundary of Bruch's membrane (BrM) to approximately 20 µm below the outer boundary of BrM. The maximum projection was applied on the segmented volumes to generate the en face angiograms. Compensation for signal loss due to the overlying anatomy on CC angiograms was achieved by using the corresponding en face CC structural image, as previously described.[27] The retinal vessel projection artifacts were removed before the identification of FDs in CC.[23] The FDs were then segmented by using a global thresholding algorithm, followed by removal

Investigative Ophthalmology & Visual Science

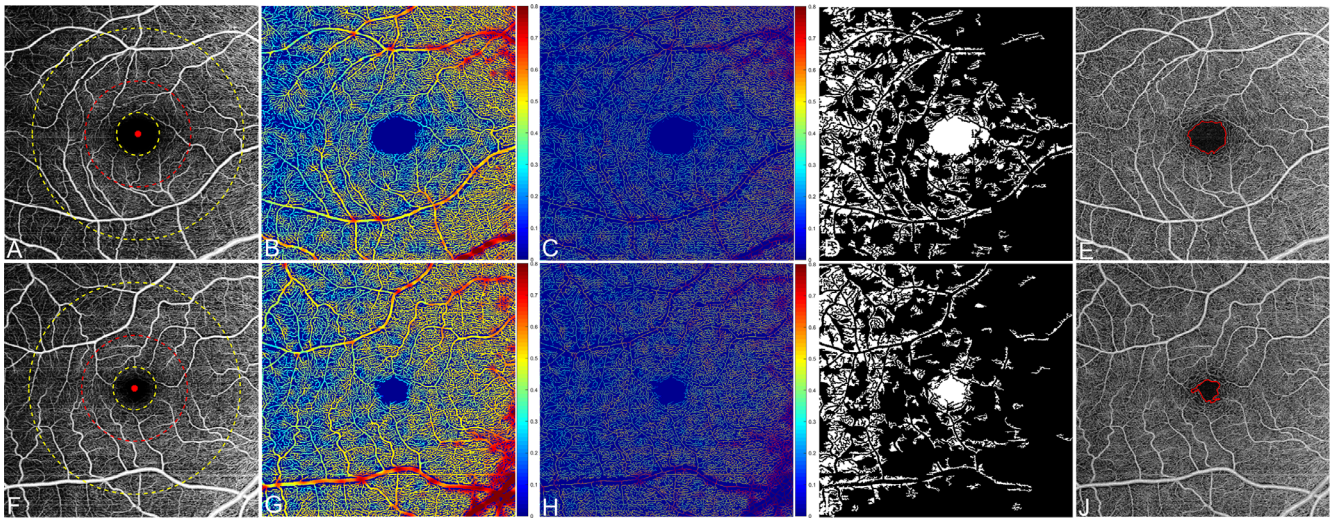

Figure 2. Representative SS-OCTA 6 × 6-mm images of superficial retinal layer and regions used for quantification. (**A**, **F**) En face superficial retinal layer OCTA images where a 1.0-mm-diameter circle (*yellow*), a 2.5-mm-diameter circle (*red*), and a 5.0-mm-diameter circle (*yellow*) centered on the fovea were overlaid, which provides specific regions used for quantification: the rim with inner and outer ring diameters of 1.0 and 2.5 mm ($R_{1.5}$, or parafovea), the rim with inner and outer ring diameters of 2.5 and 5.0 mm ($R_{2.5}$, or perifovea), and the rim with inner and outer ring diameters of 1.0 and 5.0 mm ($R_{4.0}$). (**B**, **G**) Corresponding VAD maps. (**C**, **H**) Corresponding vascular length density (VLD) maps. (**D**, **I**) Corresponding NPA maps. (**E**, **J**) Delineation of the FAZ. (**A–E**) Images are from a 61-year-old control patient. (**F–J**) Images are from a 61-year-old diabetic patient.

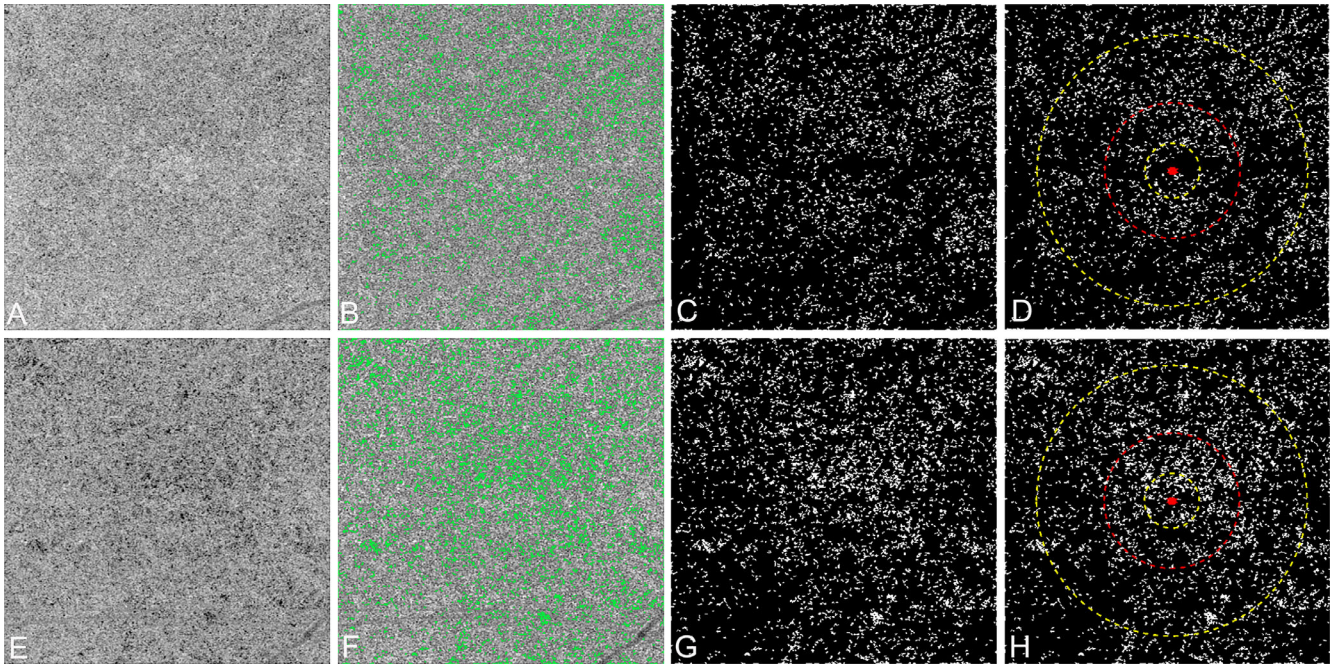

Figure 3. Representative SS-OCTA 6 × 6-mm images of CC showing FDs and the regions used for quantification. (**A**, **E**) En face CC flow OCTA images after artifact removal and structural compensation. (**B**, **F**) Corresponding FDs (*green*) overlaid onto the CC image (*gray*). (**C**, **G**) Corresponding CC FD binary maps where the *white areas* indicate the FDs. (**D**, **H**) Showing regions on CC FD binary map for quantification where the marks are given for a 1.0-mm-diameter circle (*yellow*), a 2.5-mm-diameter circle (*red*), and a 5.0-mm-diameter circle (*yellow*) centered on the fovea, resulting in four regions used for quantification: the 5.0-mm disk ($D_{5.0}$), 1.0-mm disk ($D_{1.0}$), 1.5-mm inner rim from the 1.0-mm circle to the 2.5-mm circle ($R_{1.5}$), and 2.5-mm outer rim from the 2.5-mm circle to the 5.0-mm circle ($R_{2.5}$). (**A–H**) Images are from the same patients as in Figure 2. (**A–D**) Images are from a 61-year-old control patient. (**E–H**) Images are from a 61-year-old diabetic patient.

of the FDs with a size that is smaller than the normal intercapillary distance of 24 µm.[28] The percentage of flow deficits (FD%) was calculated by the ratio between the total area of FDs and the whole area of the study region. The average size of the FDs was calculated as the total area of FDs divided by the number of FDs. Both measurements were conducted in $D_{1.0}$, $R_{1.5}$, $R_{2.5}$, and the entire 5.0-mm disk ($D_{5.0}$) (Fig. 3).

Investigative Ophthalmology & Visual Science

Table 1. Comparison of Vessel Area Density, Vessel Skeleton Density, and Nonperfusion Area Measurements in Three Retinal Layers Within Different Regions in Diabetic Eyes Without Retinopathy and Controls

	Mean ± SD Vessel Area Density (Range)		Mean ± SD Vessel Skeleton Density (Range)		Mean ± SD Nonperfusion Area (Range), mm^2	
Groups	**$R_{1.5}$**	**$R_{2.5}$**	**$R_{1.5}$**	**$R_{2.5}$**	**$R_{1.5}$**	**$R_{2.5}$**
Superficial retinal layer						
Controls	0.44 ± 0.02 (0.39 – 0.49)	0.48 ± 0.02 (0.45 – 0.52)	0.12 ± 0.01 (0.10 – 0.13)	0.13 ± 0.01 (0.12 – 0.14)	0.54 ± 0.28 (0.22 – 1.24)	1.61 ± 0.46 (1.02 – 2.76)
Diabetics	0.45 ± 0.02 (0.42 – 0.50)	0.49 ± 0.02 (0.46 – 0.54)	0.12 ± 0.01 (0.12 – 0.14)	0.13 ± 0.00 (0.12 – 0.14)	0.46 ± 0.23 (0.08 – 0.91)	1.67 ± 0.67 (0.76 – 3.04)
P value	0.186*	0.190*	0.897†	0.665*	0.590†	0.753*
Intermediate retinal layer						
Controls	0.48 ± 0.02 (0.45 – 0.51)	0.49 ± 0.02 (0.46 – 0.52)	0.12 ± 0.00 (0.12 – 0.13)	0.13 ± 0.00 (0.12 – 0.13)	0.40 ± 0.14 (0.14 – 0.65)	1.82 ± 0.66 (1.04 – 3.03)
Diabetics	0.50 ± 0.04 (0.46 – 0.63)	0.49 ± 0.03 (0.46 – 0.56)	0.13 ± 0.01 (0.12 – 0.15)	0.13 ± 0.01 (0.12 – 0.15)	0.31 ± 0.14 (0.10 – 0.65)	1.87 ± 0.49 (1.11 – 2.99)
P value	0.138†	0.752†	0.051†	1.000†	0.065*	0.777*
Deep retinal layer						
Controls	0.48 ± 0.03 (0.44 – 0.54)	0.50 ± 0.02 (0.47 – 0.53)	0.12 ± 0.01 (0.11 – 0.14)	0.13 ± 0.00 (0.12 – 0.14)	0.45 ± 0.23 (0.11 – 0.77)	0.84 ± 0.38 (0.29 – 1.62)
Diabetics	0.52 ± 0.07 (0.44 – 0.75)	0.52 ± 0.03 (0.49 – 0.62)	0.13 ± 0.01 (0.11 – 0.15)	0.13 ± 0.01 (0.12 – 0.15)	0.41 ± 0.33 (0.02 – 1.21)	0.99 ± 0.54 (0.25 – 2.48)
P value	0.110†	0.138†	0.135*	0.287†	0.287†	0.368*

Data are mean ± standard deviation unless otherwise indicated.
* By *t*-test.
† By Mann-Whitney *U* test.

Statistical Analysis

All quantitative variables were reported as means, standard deviations (SDs), and ranges. Variable normality was inspected using histograms and the Shapiro-Wilk test. Student's *t*-test or Mann-Whitney *U* test was conducted to investigate differences in continuous variables between diabetics and controls based on variable normality. The statistical analyses were performed with IBM-SPSS software version 25.0 (IBM Corporation, Armonk, New York, NY, USA). A *P* value of less than 0.05 was considered statistically significant.

Results

Sixteen eyes from 16 diabetic patients without clinically detectable retinopathy and 16 age-matched control eyes were included in this study. The populations did not show a significant difference in sex (with DM, 6 women and 10 men; without DM, 7 women and 9 men). The mean age of the participants was 61.6 ± 14.6 years (range, 22–78 years) in DM group and 61.8 ± 14.9 years (range, 22–80 years) in the control group. Mean duration of diabetes was 2.1 ± 1.2 years (range, 1–5 years). Mean glycosylated hemoglobin level in diabetic patients was 6.4% ± 0.9% (range, 5.0%–8.0%). Mean systolic blood pressure was 124.3 ± 5.1 mm Hg for controls and 126.4 ± 3.9 mm Hg for diabetics. Mean diastolic blood pressure was 73.4 ± 3.4 mm Hg for controls and 72.9 ± 7.1 mm Hg for diabetics. There was no significant difference in blood pressure measurements between the two groups ($P = 0.138$ and $P = 1.000$, respectively). In diabetic patients, there was one individual diagnosed with type 1 DM and the remaining individuals with type 2 DM.

Quantitative measurements of VAD, VSD, and NPA in the SRL, IRL, and DRL are shown in Table 1. There was no significant difference in these metrics between the controls and diabetes within all regions ($R_{1.5}$ and $R_{2.5}$, all $P > 0.05$). While the mean area of FAZ in diabetic eyes (mean, 0.38 ± 0.15 mm^2; range, 0.21–0.81 mm^2) is slightly larger than that in control eyes (mean, 0.29 ± 0.15 mm^2; range, 0.08–0.69 mm^2), no significant difference was observed between them ($P = 0.060$).

The FD% and average size of the FDs within quantified regions in CC are displayed in Table 2. Mean FD% in CC was significantly increased in diabetic eyes compared with controls within $D_{1.0}$ (23.72% vs. 16.06%; $P = 0.011$), $R_{1.5}$ (16.60% vs. 12.15%; $P = 0.003$), $R_{2.5}$ (11.04% vs. 8.29%; $P = 0.018$), and $D_{5.0}$ (12.81% vs. 9.46%; $P = 0.009$) regions. Similar findings were observed on the average size of FDs. There was significantly increased FD size within $D_{1.0}$ (3066.23 vs. 2088.34 μm^2; $P = 0.017$), $R_{1.5}$ (2147.86 vs. 1731.99 μm^2; $P = 0.009$), $R_{2.5}$ (1777.83 vs. 1497.02 μm^2; $P = 0.020$), and $D_{5.0}$ (2020.10 vs. 1651.23 μm^2; $P = 0.008$) regions in diabetic eyes compared with controls.

Discussion

The current study used a commercially available SS-OCTA to investigate the retinal and CC blood perfusion in diabetic eyes without clinically visible DR and compared their quantitative indices with those of nondiabetic controls. The diabetic eyes included in this study were from patients recently diagnosed with DM (between 1 and 5 years), and the quantitative assessments demonstrated that the CC flow reduction may precede the retinal flow changes in the macula. This finding may suggest that flow deficits in the choriocapillaris might be an earlier preclinical marker of microvascular dysfunction than retinal microvasculature in diabetic eye disease.

Investigative Ophthalmology & Visual Science

Table 2. Comparison of Percentage and Average Size of Flow Deficits Measurements in Choriocapillaris Within Different Regions in Diabetic Eyes Without Retinopathy and Controls

	Mean ± SD Percentage of Flow Deficits (Range)				Mean ± SD Average Size of Flow Deficits (Range), μm²			
Groups	**$D_{1.0}$**	**$R_{1.5}$**	**$R_{2.5}$**	**$D_{5.0}$**	**$D_{1.0}$**	**$R_{1.5}$**	**$R_{2.5}$**	**$D_{5.0}$**
Controls	16.06 ± 7.45 (3.82 – 28.89)	12.15 ± 3.96 (4.87 – 19.88)	8.29 ± 2.64 (3.12 – 12.87)	9.46 ± 2.95 (3.96 – 14.93)	2088.34 ± 768.86 (979.02 – 3585.58)	1731.99 ± 314.48 (1236.84 – 2273.87)	1497.02 ± 238.92 (1198.75 – 1937.51)	1651.23 ± 280.45 (1253.60 – 2110.55)
Diabetics	23.72 ± 8.59 (0.88 – 36.82)	16.60 ± 4.59 (3.90 – 24.90)	11.04 ± 3.51 (2.74 – 16.61)	12.81 ± 3.75 (2.92 – 18.56)	3066.23 ± 1346.99 (778.20 – 6033.12)	2147.86 ± 500.09 (1136.27 – 3220.87)	1777.83 ± 388.12 (1048.08 – 2602.22)	2020.10 ± 441.58 (1080.72 – 2779.87)
P value	0.011*	0.003†	0.018*	0.009*	0.017*	0.009*	0.020*	0.008*

Data are mean ± standard deviation unless otherwise indicated.
* By *t*-test.
† By Mann-Whitney *U* test.

Using OCTA to assess the retinal vascular density in diabetic eyes without clinically visible DR, researchers have drawn mixed conclusions. For example, Dimitrova et al.[16] and Hwang et al.[29] showed significantly reduced parafoveal VAD in both the superficial and deep retinal capillary plexuses in diabetic eyes without retinopathy compared to controls, while Simonett et al.[30] and Carnevali et al.[15] reported significantly reduced parafoveal VAD in the deep but not in the superficial plexus in diabetic eyes without retinopathy. In contrast, other groups demonstrated that no significant differences were found in the superficial, deep, or whole parafoveal VAD between the two groups.[13,14] Compared with VAD, VSD is a more sensitive metric to measure perfusion changes at the capillary level.[24] However, VSD has not been compared between diabetic patients without retinopathy and nondiabetic controls. Although OCT and histology studies have confirmed the trilaminar capillary layout in the parafovea and perifovea,[20,21,31] most of the published studies investigating vessel density separated the retinal vascular system into two major plexuses. Moreover, recent studies also showed that additional segmentation and evaluation of the intermediate retinal layer from the superficial and deep retinal layers may enhance the ability of OCTA to detect early microvascular changes in diabetic eyes.[29,32,33] In this study, VAD and VSD were measured on the SRL, IRL, and DRL using our validated semiautomated segmentation algorithm. Our study showed that no significant difference was found in VSD or VAD in diabetic eyes without retinopathy compared to controls within the three vascular plexuses for a 6 × 6-mm scanning protocol.

The FAZ area assessed by OCTA has also been well investigated in diabetic eyes without retinopathy. Some groups reported a small but significant enlargement of the FAZ area in diabetic eyes without retinopathy compared to controls,[16,34] while others reported no significant difference of FAZ between the two groups.[13–15,35–37] All of the aforementioned measurements were conducted using the built-in default settings of commercial systems with automatic segmentation into two slabs (superficial and deep). Because of inherent errors in automatic segmentation of the superficial and deep capillary plexuses within the central fovea, FAZ measurements using default settings are likely to be biased.[38] We measured the FAZ area by utilizing the full-thickness retinal slab at the edge of the FAZ where the retinal vascular plexuses merge,[22] rather than attempting to divide it artificially. Our study showed no statistically significant difference in the FAZ area between the two groups, which was consistent with recent reports.[29,36] However, another report found a small enlargement of the FAZ measured on the full-thickness slab in diabetic eyes without retinopathy.[39] Further studies with larger sample sizes are needed to evaluate whether FAZ measurements would be a useful diagnostic tool for early diabetic microvascular dysfunction.

Retinal nonperfusion area (NPA) measurements were reported as a sensitive OCTA quantitative metric and could distinguish diabetic eyes without retinopathy from normal eyes.[29,36] We also conducted a detailed investigation into the NPA; however, in our study, no statistical difference of the NPA was observed in the parafoveal or perifoveal region between the two groups in different retinal layers. One possibility for the discrepancy in the results is that in contrast to the earlier study, our diabetic cohort had a short duration from diagnosis of DM (2.1 ± 1.2 years), which may have allowed us to study the microvascular changes in diabetic eyes at a very early stage. Furthermore, although the NPA was reported to be less age dependent,[40] we nevertheless selected age-matched individuals as controls in this study since prior investigations have shown that vascular density,[41–43] FAZ size,[41,43] and CC FDs tended to be influenced by age.[44,45]

Several groups also investigated CC perfusion in diabetic eyes. Using an investigational SS-OCT system, Choi et al.[46] described focal or diffuse CC flow impairment in diabetic eyes without quantitative assessments. Nesper et al.[13] reported increased percent area of nonperfusion in CC in a 3 × 3-mm angiogram in diabetic eyes without retinopathy using a commercially available SD-OCT system. On the other hand, other groups reported no significant difference in CC vessel density between diabetic eyes without retinopathy and normal controls with SD-OCTA.[14–16] However, the vessel density metric may not be a good choice for CC quantification. As we know, CC vasculature is extremely dense in the posterior pole with small intercapillary distances (5–20 µm) that are smaller than the OCT system's lateral resolution (15–20 µm)[47]; therefore, individual capillaries of CC cannot be clearly resolved with current commercial OCT systems. Instead of quantifying the CC vasculature directly, many researchers have chosen flow deficits to analyze CC perfusion.[12,44,45] The CC FD represents the area where there is a lack of CC flow or CC flow below the detectable threshold of the OCT system. To improve the robust assessment of the CC FDs, we segmented FDs with a size larger than normal intercapillary spacing (24 μm in diameter) for quantification, which is within the capability of the OCT system to resolve.[28] Moreover, we quantitated and compared the CC FDs in different macular regions since the CC FDs presented regional distributions in the macula.[44,45] We observed significantly increased FD% and enlarged average size of FDs in CC in diabetic eyes compared with controls within all quantified regions.

Vascular abnormalities in the choriocapillaris have also been demonstrated in diabetic eyes without retinopathy in histopathologic studies. Using alkaline phosphatase activity as a marker for viable CC endothelial cells, McLeod and Lutty[48] found that CC dropout was generally much more pronounced and involved larger areas in postmortem subjects with diabetes even without DR than those without diabetes. Interestingly, in a mouse model of DM, reduced choroidal perfusion was noted to occur prior to alterations of retinal perfusion and visual function.[49] Impaired visual function preceding clinically visible DR has also been observed in some population-based studies.[50,51] In the present study, we demonstrated with noninvasive SS-OCTA that CC perfusion reduction may precede retinal vascular changes in the macula of diabetic eyes. Although the outer retina receives most of its blood supply from the CC,[52] whether reduced perfusion contributes to abnormal visual function in diabetic patients before overt retinopathy still requires further investigation.

We acknowledge several limitations in this study. First, our study included a relatively small number of patients. This was mainly related to the strict exclusion criteria we employed. Larger cohort studies are necessary to confirm these preliminary findings. Second, this is a cross-sectional analysis with a short duration of diabetes. With the increase of duration, choroidal and retinal microvascular alterations may be more obvious and present different characteristics. Further longitudinal studies are needed to elucidate these microvascular alterations over time with the progression of diabetes. Third, no significant changes in retinal perfusion

metrics were observed between the two groups. However, this does not necessarily mean that early retinal vascular alterations are not actually present. The development of more sensitive OCTA metrics may help to detect retinal perfusion alterations in early diabetes. Fourth, imaging of the deep large choroidal vessels may also provide additional information on the pathogenesis and progression of diabetic eye disease, which warrants a proper investigation. Lastly, we did not correct image magnification in lateral measurements due to the variation of axial length.[53] The magnification variation may affect the ability of the quantification metrics of FAZ, NPA, and CC FD sizes, although it has a negligible effect on the density or percentage measurements (e.g., VAD, VSD, and CC FD%). In the current study, only the patients with a refraction error less myopic than –6.0 diopters were included for the analyses. This inclusion criterion would limit the magnification variation to a relatively small range. This study was retrospective in its nature, and axial length measurements were not available for all the patients. Nevertheless, we ran a test on the FAZ, NPA, and mean size of FDs by considering the magnification variation and assuming the axial length artificially at the extreme cases of 26.4 mm (–6.0 diopters) and found that this did not change our final conclusions. However, we would suggest in future larger cohort and longitudinal studies that this magnification factor is considered for more accurate analyses to draw more definitive conclusions, particularly in the cases of myopic/hyperopic eyes.

Conclusions

Noninvasive, in vivo SS-OCTA imaging revealed that perfusion of the choriocapillaris is significantly decreased in diabetic patients without retinopathy compared with age-matched nondiabetic controls. This decrease in CC perfusion was noted despite an absence of macular retinal vessel parameter changes. Decreased CC perfusion in the macula may be an early indicator of otherwise clinically undetectable diabetic vasculopathy. Further larger longitudinal studies are needed to confirm these findings and elucidate microvascular alterations over time in diabetic eyes.

Acknowledgments

Supported by grants from Carl Zeiss Meditec, Inc. (Dublin, CA, USA), the National Eye Institute (R01EY028753), and an unrestricted grant from the Research to Prevent Blindness, Inc. (New York, NY, USA). The funding organization had no role in the design or conduct of this research.

Disclosure: **Y. Dai**, None; **H. Zhou**, None; **Z. Chu**, None; **Q. Zhang**, None; **J.R. Chao**, None; **K.A. Rezaei**, None; **R.K. Wang**, Carl Zeiss Meditec, Inc. (C, F, P), Insight Photonic Solutions (C)

References

1. Moss SE, Klein R, Klein BE. The 14-year incidence of visual loss in a diabetic population. *Ophthalmology*. 1998;105:998–1003.
2. Cheung N, Mitchell P, Wong TY. Diabetic retinopathy. *Lancet*. 2010;376:124–136.
3. Ting DS, Cheung GC, Wong TY. Diabetic retinopathy: global prevalence, major risk factors, screening practices and public health challenges: a review. *Clin Exp Ophthalmol*. 2016;44:260–277.
4. Safi H, Safi S, Hafezi-Moghadam A, Ahmadieh H. Early detection of diabetic retinopathy. *Surv Ophthalmol*. 2018;63:601–608.
5. Stitt AW, Curtis TM, Chen M, et al. The progress in understanding and treatment of diabetic retinopathy. *Prog Retin Eye Res*. 2016;51:156–186.
6. Campos A, Campos EJ, Martins J, Ambrosio AF, Silva R. Viewing the choroid: where we stand, challenges and contradictions in diabetic retinopathy and diabetic macular oedema. *Acta Ophthalmol*. 2017;95:446–459.
7. Hua R, Liu L, Wang X, Chen L. Imaging evidence of diabetic choroidopathy in vivo: angiographic pathoanatomy and choroidal-enhanced depth imaging. *PLoS One*. 2013;8:e83494.
8. Shiragami C, Shiraga F, Matsuo T, Tsuchida Y, Ohtsuki H. Risk factors for diabetic choroidopathy in patients with diabetic retinopathy. *Graefes Arch Clin Exp Ophthalmol*. 2002;240:436–442.
9. Weinberger D, Kramer M, Priel E, Gaton DD, Axer-Siegel R, Yassur Y. Indocyanine green angiographic findings in nonproliferative diabetic retinopathy. *Am J Ophthalmol*. 1998;126:238–247.
10. Yannuzzi LA, Sorenson JA, Guyer DR, Slakter JS, Chang B, Orlock D. Indocyanine green videoangiography: current status. *Eur J Ophthalmol*. 1994;4:69–81.
11. Fujimoto J, Swanson E. The development, commercialization, and impact of optical coherence tomography. *Invest Ophthalmol Vis Sci*. 2016;57:OCT1–OCT13.
12. Spaide RF, Fujimoto JG, Waheed NK, Sadda SR, Staurenghi G. Optical coherence tomography angiography. *Prog Retin Eye Res*. 2018;64:1–55.
13. Nesper PL, Roberts PK, Onishi AC, et al. Quantifying microvascular abnormalities with increasing severity of diabetic retinopathy using optical coherence tomography angiography. *Invest Ophthalmol Vis Sci*. 2017;58:BIO307–BIO315.
14. Conti FF, Qin VL, Rodrigues EB, et al. Choriocapillaris and retinal vascular plexus density of diabetic eyes using split-spectrum amplitude decorrelation spectral-domain optical coherence tomography angiography. *Br J Ophthalmol*. 2019;103:452–456.
15. Carnevali A, Sacconi R, Corbelli E, et al. Optical coherence tomography angiography analysis of retinal vascular plexuses and choriocapillaris in patients with type 1 diabetes without diabetic retinopathy. *Acta Diabetol*. 2017;54:695–702.
16. Dimitrova G, Chihara E, Takahashi H, Amano H, Okazaki K. Quantitative retinal optical coherence tomography angiography in patients with diabetes without diabetic retinopathy. *Invest Ophthalmol Vis Sci*. 2017;58:190–196.
17. Chen CL, Wang RK. Optical coherence tomography based angiography [Invited]. *Biomed Opt Express*. 2017;8:1056–1082.
18. Wang RK, An L, Francis P, Wilson DJ. Depth-resolved imaging of capillary networks in retina and choroid using ultrahigh sensitive optical microangiography. *Opt Lett*. 2010;35:1467–1469.
19. Yin X, Chao JR, Wang RK. User-guided segmentation for volumetric retinal optical coherence tomography images. *J Biomed Opt*. 2014;19:086020.
20. Chan G, Balaratnasingam C, Yu PK, et al. Quantitative morphometry of perifoveal capillary networks in the human retina. *Invest Ophthalmol Vis Sci*. 2012;53:5502–5514.
21. Yu DY, Cringle SJ, Yu PK, et al. Retinal capillary perfusion: spatial and temporal heterogeneity. *Prog Retin Eye Res*. 2019;70:23–54.
22. Snodderly DM, Weinhaus RS, Choi JC. Neural-vascular relationships in central retina of macaque monkeys (*Macaca fascicularis*). *J Neurosci*. 1992;12:1169–1193.

23. Zhang A, Zhang Q, Wang RK. Minimizing projection artifacts for accurate presentation of choroidal neovascularization in OCT micro-angiography. *Biomed Opt Express*. 2015;6:4130–4143.
24. Chu Z, Lin J, Gao C, et al. Quantitative assessment of the retinal microvasculature using optical coherence tomography angiography. *J Biomed Opt*. 2016;21:66008.
25. Kim AY, Rodger DC, Shahidzadeh A, et al. Quantifying retinal microvascular changes in uveitis using spectral-domain optical coherence tomography angiography. *Am J Ophthalmol*. 2016;171:101–112.
26. Kim AY, Chu Z, Shahidzadeh A, Wang RK, Puliafito CA, Kashani AH. Quantifying microvascular density and morphology in diabetic retinopathy using spectral-domain optical coherence tomography angiography. *Invest Ophthalmol Vis Sci*. 2016;57:OCT362–OCT370.
27. Zhang Q, Zheng F, Motulsky EH, et al. A novel strategy for quantifying choriocapillaris flow voids using swept-source OCT angiography. *Invest Ophthalmol Vis Sci*. 2018;59:203–211.
28. Zhang Q, Shi Y, Zhou H, et al. Accurate estimation of choriocapillaris flow deficits beyond normal intercapillary spacing with swept source OCT angiography. *Quant Imaging Med Surg*. 2018;8:658–666.
29. Hwang TS, Hagag AM, Wang J, et al. Automated quantification of nonperfusion areas in 3 vascular plexuses with optical coherence tomography angiography in eyes of patients with diabetes. *JAMA Ophthalmol*. 2018;136:929–936.
30. Simonett JM, Scarinci F, Picconi F, et al. Early microvascular retinal changes in optical coherence tomography angiography in patients with type 1 diabetes mellitus. *Acta Ophthalmol*. 2017;95:e751–e755.
31. Nesper PL, Fawzi AA. Human parafoveal capillary vascular anatomy and connectivity revealed by optical coherence tomography angiography. *Invest Ophthalmol Vis Sci*. 2018;59:3858–3867.
32. Park JJ, Soetikno BT, Fawzi AA. Characterization of the middle capillary plexus using optical coherence tomography angiography in healthy and diabetic eyes. *Retina*. 2016;36:2039–2050.
33. Onishi AC, Nesper PL, Roberts PK, et al. Importance of considering the middle capillary plexus on OCT angiography in diabetic retinopathy. *Invest Ophthalmol Vis Sci*. 2018;59:2167–2176.
34. Takase N, Nozaki M, Kato A, Ozeki H, Yoshida M, Ogura Y. Enlargement of foveal avascular zone in diabetic eyes evaluated by en face optical coherence tomography angiography. *Retina*. 2015;35:2377–2383.
35. Lee H, Lee M, Chung H, Kim HC. Quantification of retinal vessel tortuosity in diabetic retinopathy using optical coherence tomography angiography. *Retina*. 2018;38:976–985.
36. Lu Y, Simonett JM, Wang J, et al. Evaluation of automatically quantified foveal avascular zone metrics for diagnosis of diabetic retinopathy using optical coherence tomography angiography. *Invest Ophthalmol Vis Sci*. 2018;59:2212–2221.
37. Goudot MM, Sikorav A, Semoun O, et al. Parafoveal OCT angiography features in diabetic patients without clinical diabetic retinopathy: a qualitative and quantitative analysis. *J Ophthalmol*. 2017;2017:8676091.
38. Spaide RF, Curcio CA. Evaluation of segmentation of the superficial and deep vascular layers of the retina by optical coherence tomography angiography instruments in normal eyes. *JAMA Ophthalmol*. 2017;135:259–262.
39. de Carlo TE, Chin AT, Bonini Filho MA, et al. Detection of microvascular changes in eyes of patients with diabetes but not clinical diabetic retinopathy using optical coherence tomography angiography. *Retina*. 2015;35:2364–2370.
40. Zhang M, Hwang TS, Dongye C, Wilson DJ, Huang D, Jia Y. Automated quantification of nonperfusion in three retinal plexuses using projection-resolved optical coherence tomography angiography in diabetic retinopathy. *Invest Ophthalmol Vis Sci*. 2016;57:5101–5106.
41. Iafe NA, Phasukkijwatana N, Chen X, Sarraf D. Retinal capillary density and foveal avascular zone area are age-dependent: quantitative analysis using optical coherence tomography angiography. *Invest Ophthalmol Vis Sci*. 2016;57:5780–5787.
42. Lavia C, Bonnin S, Maule M, Erginay A, Tadayoni R, Gaudric A. Vessel density of superficial, intermediate, and deep capillary plexuses using optical coherence tomography angiography. *Retina*. 2019;39:247–258.
43. Garrity ST, Iafe NA, Phasukkijwatana N, Chen X, Sarraf D. Quantitative analysis of three distinct retinal capillary plexuses in healthy eyes using optical coherence tomography angiography. *Invest Ophthalmol Vis Sci*. 2017;58:5548–5555.
44. Zheng F, Zhang Q, Shi Y, et al. Age-dependent changes in the macular choriocapillaris of normal eyes imaged with swept-source OCT angiography. *Am J Ophthalmol*. 2019;200:110–122.
45. Nassisi M, Baghdasaryan E, Tepelus T, Asanad S, Borrelli E, Sadda SR. Topographic distribution of choriocapillaris flow deficits in healthy eyes. *PLoS One*. 2018;13:e0207638.
46. Choi W, Waheed NK, Moult EM, et al. Ultrahigh speed swept source optical coherence tomography angiography of retinal and choriocapillaris alterations in diabetic patients with and without retinopathy. *Retina*. 2017;37:11–21.
47. Olver JM. Functional anatomy of the choroidal circulation: methyl methacrylate casting of human choroid. *Eye (Lond)*. 1990;4:262–272.
48. McLeod DS, Lutty GA. High-resolution histologic analysis of the human choroidal vasculature. *Invest Ophthalmol Vis Sci*. 1994;35:3799–3811.
49. Muir ER, Renteria RC, Duong TQ. Reduced ocular blood flow as an early indicator of diabetic retinopathy in a mouse model of diabetes. *Invest Ophthalmol Vis Sci*. 2012;53:6488–6494.
50. Sokol S, Moskowitz A, Skarf B, Evans R, Molitch M, Senior B. Contrast sensitivity in diabetics with and without background retinopathy. *Arch Ophthalmol*. 1985;103:51–54.
51. Katz G, Levkovitch-Verbin H, Treister G, Belkin M, Ilany J, Polat U. Mesopic foveal contrast sensitivity is impaired in diabetic patients without retinopathy. *Graefes Arch Clin Exp Ophthalmol*. 2010;248:1699–1703.
52. Bhutto I, Lutty G. Understanding age-related macular degeneration (AMD): relationships between the photoreceptor/retinal pigment epithelium/Bruch's membrane/choriocapillaris complex. *Mol Aspects Med*. 2012;33:295–317.
53. Sampson DM, Gong P, An D, et al. Axial length variation impacts on superficial retinal vessel density and foveal avascular zone area measurements using optical coherence tomography angiography. *Invest Ophthalmol Vis Sci*. 2017;58:3065–3072.

Investigative Ophthalmology & Visual Science